

Corticospinal tract conduction block results in the prolongation of central motor conduction time in compressive cervical myelopathy

Kazuyoshi Nakanishi*, Nobuhiro Tanaka, Yasushi Fujiwara, Naosuke Kamei, Mitsuo Ochi

Department of Orthopaedic Surgery, Programs for Applied Biomedicine, Division of Clinical Medical Science, Graduate School of Biomedical Sciences, Hiroshima University, Kasumi 1-2-3, Minami-ku, Hiroshima 734-8551, Japan

* Corresponding author. Tel.: +81-82-257-5232; fax: +81-82-257-5234. E-mail address: kazn@hiroshima-u.ac.jp (K. Nakanishi)

Abstract

Objective: The objective of this study was to analyze corticospinal function in patients with compressive cervical myelopathy and to elucidate the mechanism underlying its prolonged central motor conduction time (CMCT).

Methods: Motor evoked potentials following transcranial magnetic stimulation (TMS) and peripheral conduction time in the ulnar and tibial nerves following electrical stimulation were measured from the abductor digiti minimi (ADM) and abductor hallucis (AH) muscles in 24 patients with compressive cervical myelopathy and used to calculate CMCT. Spinal cord evoked potentials (SCEPs) following transcranial electric stimulation were recorded intraoperatively from the C2-3 to C6-7 intervertebral levels. Correlations between prolonged CMCT and SCEP values were then estimated.

Results: The shorter/longer CMCT between the patients' right and left ADM and AH were $8.5 \pm 2.9/11.5 \pm 3.3$ and $16.2 \pm 3.1/18.4 \pm 3.3$ ms, respectively (mean \pm SD). The SCEPs amplitude at C6-7, compared to C2-3, was 25.7 ± 21.0 %. The attenuation of SCEP amplitude, but not latency, at C6-7 correlated significantly with CMCT prolongation.

Conclusions: Our data support the view that CMCT prolongation is primarily due to corticospinal conduction block, rather than conduction delay.

Significance: Insight was provided into the mechanism of corticospinal dysfunction in compressive cervical myelopathy.

Keywords: motor evoked potentials; central motor conduction time; spinal cord evoked potentials; cervical myelopathy; transcranial magnetic stimulation

1. Introduction

Measurement of motor evoked potentials (MEPs) following transcranial magnetic stimulation (TMS) is a noninvasive, useful means to evaluate the electrophysiologic function of the corticospinal tract (Jaskolski et al., 1989; Maertens de Noordhout et al., 1991). In particular, measurement of central motor conduction time (CMCT) can be used to electrophysiologically evaluate corticospinal function in compressive cervical myelopathy (Di Lazzaro et al., 1992; Tavy et al., 1994; Ofuji et al., 1998; Kaneko et al., 2001). In fact, an excellent correlation was reported between magnetic resonance imaging (MRI) findings and CMCT in patients with cervical myelopathy (Lo et al., 2004). Specifically, CMCT was found to be more prolonged in patients who had more severe cervical spinal cord compression as determined by MRI analysis.

CMCT is calculated by subtracting peripheral conduction time (PCT), determined by peripheral nerve stimulation, from MEP latency. Thus, the physiology of prolonged CMCT is complex and there have been only a few reports regarding the mechanism by which it occurs in cervical myelopathy. Kaneko and his colleagues (2001) examined CMCT following TMS, as well as spinal cord evoked potentials (SCEPs) following transcranial electric stimulation (TES) in patients with compressive cervical myelopathy and normal subjects. Their results showed that CMCT was prolonged in such patients and that they exhibited a significant attenuation in their SCEP amplitudes following TES, but no significant delay in their SCEP latencies. Thus, they concluded that impaired temporal summation of multiple descending potentials following TMS produced delays in motor neuron firing that contributed to the prolongation of CMCT.

In light of the above data, we hypothesized that there may be a correlation between the degree of conduction block and the prolongation of CMCT in these patients. To examine this, we analyzed a series of 24 compressive cervical myelopathy patients who underwent both MEP recordings for CMCT measurement preoperatively, and SCEP recordings after TES during surgery.

2. Materials and Methods

2.1. Patients with compressive cervical myelopathy

Twenty four patients (9 women and 15 men) with compressive cervical myelopathy that were treated in our department between September 2003 and August 2004 were included in this study. Patients with other brain, thoracic spinal cord, cauda equina, or peripheral nerve disorders were excluded. Their mean age was 65 years (range 36-81 years) and their mean height was 159 cm (range 136-173 cm). All patients provided informed consent prior to the initiation of the study.

All of the above subjects exhibited a sensory disturbance in their upper and/or lower limbs, and had a spastic gait disturbance. The presence of compressive cervical myelopathy was confirmed by neurological testing and MRI, and was found to have been due to either cervical spondylosis (16 patients), ossification of the posterior longitudinal ligament (OPLL; 4 patients), or cervical disc herniation (4 patients). All patients underwent laminoplasty after which some exhibited neurological improvement. None of these subjects exhibited any abnormalities in their sensory or motor peripheral nerve conduction velocities.

T2 weighted (repetition pulse 3000 ms, echo time 120 ms) MRI (SIGNA 1.5 Tesla device; GE Yokogawa Medical Systems, Tokyo, Japan) was used to determine, in

a blinded fashion by a roentgenologist and two orthopedic surgeons, the levels at which the spinal cord was most severely compressed. Inter-observer agreement (κ) vis-à-vis the patients' MRI findings was 0.899; since the agreement ratio was high, one of the three assessments was randomly selected and used for data analysis.

2.2. Measurement of CMCT

Surface recording electrodes were bilaterally placed on the abductor digiti minimi (ADM) and abductor hallucis (AH) muscles using the standard belly-tendon method. TMS was delivered using a round 14-cm outer diameter coil (Model 200; Magstim, Whitland, UK), the center of which was held over the vertex of the cranium when MEP recordings were made from the ADM. A clockwise current in the coil, as viewed from above, was delivered to stimulate the left hemisphere and a counterclockwise current was used to stimulate the right hemisphere. The magnetic stimulus intensity was set at 20 % above the threshold for the MEPs. The coil was then shifted anteriorly when the MEP recordings were made from the AH muscles. The MEPs were recorded at least 4 times; all responses were superimposed and their latencies measured (Fig. 1-a, b).

Compound muscle action potentials (CMAPs) and F-waves were recorded following continuous current stimulation at supramaximal intensity (0.2 ms square wave pulses) of the ulnar and tibial nerves at the wrist and ankle, respectively. Thirty two serial responses were obtained and the shortest F-wave latency was measured.

All muscle responses were recorded using a commercially available system (Viking IV; Nicolet Biomedical, WI, USA) after they traversed a bandpass filter of 0.5-2000 Hz. An epoch of 100 ms after stimulation was digitized at a 5 kHz sampling

rate. The peripheral conduction time (PCT), excluding the turnaround time at the spinal motor neuron (1 ms), was calculated from the latencies of the CMAPs and F-waves as follows: $(\text{latency of CMAPs} + \text{latency of F-waves} - 1) / 2$ (Kimura, 1984). The conduction time from the motor cortex to the spinal motor neurons (i.e., the CMCT) was calculated by subtracting the PCT from the onset latency of the MEPS.

2.3. Recording of the SCEPs

SCEPs were recorded intraoperatively before decompression. Needle electrodes (Needle Electrode; Unique Medical, Tokyo, Japan) were inserted into the ligamentum flavum in the interlaminar space between C2-3 through C6-7, and a reference electrode was placed in the paravertebral muscles. The transcranial stimulating electrodes (Cranial Coil Electrode; Unique Medical, Tokyo, Japan) were placed subcutaneously and were used to stimulate the motor cortex electrically 5 cm lateral and 2 cm anterior to the vertex (Fig. 1-c). The anode was placed into the scalp contralateral to the side of the ADM that showed the longer CMCT i.e., the side which was more severely affected; an anodal TES current was used because it depolarizes axons and cell bodies in the motor cortex more effectively than does a cathodal current. The motor cortex was stimulated transcranially with 0.2 ms square wave pulses using a constant current of 100 mA. The SCEPs were detected from the needle electrodes following TES, and were recorded after they traversed a bandpass filter of 0.5-2000 Hz.. An epoch of 50 ms after stimulation was digitized at a 5 kHz sampling rate, and 50 responses were averaged. Latencies and amplitudes of the first negative peaks were measured at each level, according to the method of Kaneko et al (Kaneko et al., 2001). The amplitude was measured from the baseline to the first negative peak (Fig. 1-d). The amplitude ratio of the C6-7

intervertebral level compared to the amplitude at the C2-3 level was calculated.

2.4. Statistical analysis

The PCT values were evaluated between the right and left sides. Data were compared using the Mann-Whitney U test for nonparametric statistical analysis; a p value of < 0.05 was considered to be statistically significant. Correlations between the CMCT and SCEP values were estimated using the Pearson's correlation coefficient (r). A correlation was accepted as significant when $p < 0.05$ as well as $|r| > 0.4$. The electrophysiological data are presented as the mean \pm SD (range).

3. Results

3.1. CMCT calculated from MEPs and PCT

The MEP latencies from the right/left ADM and AH were 24.2 ± 3.2 (19.2-30.3)/ 24.3 ± 3.8 (19.6-33.7) ms and 43.6 ± 4.0 (38.4-50.9)/ 43.3 ± 4.9 (35.8-53.9) ms, respectively. PCTs from the right/left ADM and AH were 14.3 ± 1.9 (11.8-16.4)/ 14.3 ± 2.1 (10.9-16.3) ms and 26.1 ± 3.1 (22.0-28.4)/ 26.4 ± 3.0 (22.0-28.5) ms, respectively. There were no significant differences in PCTs from the ADM and AH between the right and left muscles. The shorter/longer CMCTs between the patients' right and left ADM and AH were 8.5 ± 2.9 (3.6-16.5)/ 11.4 ± 3.5 (6.6-17.9) ms and 16.2 ± 3.1 (10.6-22.0) / 18.2 ± 3.6 (13.5-26.6) ms, respectively.

3.2. SCEPs and their correlation to MRI findings

In all patients, only one SCEP component (D-wave; Patton and Amassian, 1954)

was recorded at the C2-3 intervertebral level. The latency and amplitude of the D-waves at this level were 3.2 ± 0.3 (2.8-3.6) ms and 35.5 ± 18.3 (14.5-64.9) μV , respectively. The intervertebral levels where the D-wave amplitude reduced most steeply compared to the immediately rostral recording were at C3-4 in 2 patients, C4-5 in 13 patients, and C5-6 in 9 patients. The amplitude at these, compared to the immediately rostral, levels was 52.0 ± 23.7 (16.1-93.6) %. The levels that displayed the most severe spinal cord compression on MRI coincided with these levels. Small D-waves with broadening that was likely due to abnormal dispersion were detected at C6-7 in 22 patients. In the remaining two patients, clear D-waves were not recorded caudal to the level that showed marked D-wave attenuation. The mean D-wave latency at C6-7 in all but two patients in whom no D-waves were recorded at C6-7 was 4.3 ± 0.4 (3.4-4.9) ms. The amplitude at C6-7 in all patients was 9.4 ± 10.3 (0-41.2) μV , and the amplitude ratio of C6-7 to C2-3 was 25.7 ± 21.0 (0-87.8) %.

3.3. Correlation between CMCT and attenuation of SCEP amplitude

The CMCT and SCEPs values are shown in Table 1. All 24 patients showed a significant correlation between their shorter/longer CMCTs and amplitude ratios of their D-waves, both from the ADM ($r = -0.54, p = 0.005/r = -0.68, p = 0.0001$) and the AH ($r = -0.45, p = 0.027/r = -0.46, p = 0.025$) (Fig. 2-a, b). However, 22 of these patients (all but the two patients who did not exhibit a clear D-wave at C6-7) did not show any correlation between their CMCTs and D-wave latencies at C6-7 (Fig. 2-c, d).

4. Discussion

Our data showed that the SCEP amplitude ratio of C6-7 to C2-3 correlated

significantly with CMCT prolongation. In contrast, no correlation between SCEP latency at the C6-7 level and CMCT prolongation was observed. The steepest reduction in SCEP amplitude, compared to the immediately rostral recording, was observed at levels that displayed the most severe compression by MRI. Significant lesions were uncovered, by MRI and by analyzing our SCEP findings, that were rostral to the segmental levels that innervated the ADM (from C6-7 to C7-T1) and AH, suggesting that the prolonged CMCT seen in these patients was not due to gray matter dysfunction but rather to corticospinal tract impairment.

Peripheral nerve conduction delay is a common abnormal finding in chronic compressive peripheral lesions (Rydevik and Nordborg, 1980; Kimura, 1984). Thus, animals with chronic nerve compression demonstrated progressive slowing of their nerve conduction velocities (O'Brien et al., 1987). Chronic peripheral nerve compression induces local demyelination and remyelination, with shortening of the inter-node distances (Ochoa et al., 1972; O'Brien et al., 1987; Gupta et al., 2004), resulting in reduced nerve conduction velocity. However, the fact that CMCT prolongation did not correlate with SCEP latency in our study suggests that the former was not caused by corticospinal conduction delay.

Conduction block of evoked spinal cord responses is an important clinical feature of compressive spinal cord lesions (Tani et al., 1999). In our study, CMCT prolongation correlated significantly with the attenuation of SCEP amplitude at C6-7, but not with the latency at C6-7. This finding suggests that CMCT prolongation was caused by more pronounced attenuation of corticospinal descending potentials in the absence of a significant conduction delay. In compressive cervical myelopathy, gray matter is preferentially damaged (Ichihara et al., 2001), resulting in the loss of neurons, necrosis,

and cavitation at the site of spinal cord compression, though white matter damage in the form of myelin destruction and the loss of axons has also been reported (Mair and Druckman, 1953; Wilkinson, 1960; al-Mefty et al., 1993; Kameyama et al., 1995). Our results showed that CMCT prolongation in the compressive cervical myelopathy primarily reflected the severity of corticospinal conduction block, which may have resulted from the loss of functional axons due to spinal cord compression.

An explanation of how CMCT prolongation might occur has been offered by Kaneko et al. (Kaneko et al., 2001), who suggested that spinal motor neurons might need more time to fire in compressive cervical myelopathy when corticospinal potentials, but not conduction, are attenuated, thereby resulting in prolonged CMCT. Impaired temporal summation of multiple descending potentials following TMS may produce delays in motor neuron firing that contribute to CMCT prolongation.

In conclusion, our data support the view that CMCT prolongation in patients with compressive cervical myelopathy is primarily due to corticospinal conduction block, rather than conduction delay.

Figure legends

Fig. 1. (a, b) MEP waveforms recorded from the ADM and AH on both sides. (c) Sites at which TES was carried out. The stimulus electrodes were placed 5 cm lateral and 2 cm anterior to the vertex. (d) SCEPs following TES recorded in a patient with compressive cervical myelopathy. The D-wave amplitudes were measured from the baseline to the first negative peak.

Fig. 2. Correlations between CMCTs and SCEPs. The black and white dots indicate the values obtained from the ADM and AH, respectively. (a, b) The (a) shorter/ (b) longer CMCTs from the ADM and the AH correlated significantly with the D-wave amplitude ratios of the C6-7 to C2-3 intervertebral levels. (c, d) Twenty two patients (i.e., all but the two patients that failed to exhibit clear D-waves at the C6-7 level) failed to demonstrate a correlation between their (c) shorter/ (d) longer CMCTs and D-wave latencies at the C6-7 level.

References

- al-Mefty O, Harkey HL, Marawi I, Haines DE, Peeler DF, Wilner HI, Smith RR, Holaday HR, Haining JL, Russell WF, et al. Experimental chronic compressive cervical myelopathy. *J Neurosurg* 1993; 79: 550-61.
- Di Lazzaro V, Restuccia D, Colosimo C, Tonali P. The contribution of magnetic stimulation of the motor cortex to the diagnosis of cervical spondylotic myelopathy. Correlation of central motor conduction to distal and proximal upper limb muscles with clinical and MRI findings. *Electroencephalogr Clin Neurophysiol* 1992; 85: 311-20.
- Gupta R, Rowshan K, Chao T, Mozaffar T, Steward O. Chronic nerve compression induces local demyelination and remyelination in a rat model of carpal tunnel syndrome. *Exp Neurol* 2004; 187: 500-8.
- Ichihara K, Taguchi T, Shimada Y, Sakuramoto I, Kawano S, Kawai S. Gray matter of the bovine cervical spinal cord is mechanically more rigid and fragile than the white matter. *J Neurotrauma* 2001; 18: 361-7.
- Jaskolski DJ, Jarratt JA, Jakubowski J. Clinical evaluation of magnetic stimulation in cervical spondylosis. *Br J Neurosurg* 1989; 3: 541-8.
- Kameyama T, Hashizume Y, Ando T, Takahashi A, Yanagi T, Mizuno J. Spinal cord morphology and pathology in ossification of the posterior longitudinal ligament. *Brain* 1995; 118 (Pt 1): 263-78.
- Kaneko K, Taguchi T, Morita H, Yonemura H, Fujimoto H, Kawai S. Mechanism of prolonged central motor conduction time in compressive cervical myelopathy. *Clin Neurophysiol* 2001; 112: 1035-40.

- Kimura J. Principles and pitfalls of nerve conduction studies. *Ann Neurol* 1984; 16: 415-29.
- Lo YL, Chan LL, Lim W, Tan SB, Tan CT, Chen JL, Fook-Chong S, Ratnagopal P. Systematic correlation of transcranial magnetic stimulation and magnetic resonance imaging in cervical spondylotic myelopathy. *Spine* 2004; 29: 1137-45.
- Maertens de Noordhout A, Remacle JM, Pepin JL, Born JD, Delwaide PJ. Magnetic stimulation of the motor cortex in cervical spondylosis. *Neurology* 1991; 41: 75-80.
- Mair WG, Druckman R. The pathology of spinal cord lesions and their relation to the clinical features in protrusion of cervical intervertebral discs; a report of four cases. *Brain* 1953; 76: 70-91.
- O'Brien JP, Mackinnon SE, MacLean AR, Hudson AR, Dellon AL, Hunter DA. A model of chronic nerve compression in the rat. *Ann Plast Surg* 1987; 19: 430-5.
- Ochoa J, Fowler TJ, Gilliatt RW. Anatomical changes in peripheral nerves compressed by a pneumatic tourniquet. *J Anat* 1972; 113: 433-55.
- Ofuji A, Kaneko K, Taguchi T, Fuchigami Y, Morita H, Kawai S. New method to measure central motor conduction time using transcranial magnetic stimulation and T-response. *J Neurol Sci* 1998; 160: 26-32.
- Patton HD, Amassian VE. Single and multi-unit analysis of cortical stage of pyramidal activation. *J Neurophysiol* 1954; 17: 345-362.
- Rydevik B, Nordborg C. Changes in nerve function and nerve fibre structure induced by acute, graded compression. *J Neurol Neurosurg Psychiatry* 1980; 43: 1070-82.

- Tani T, Yamamoto H, Kimura J. Cervical spondylotic myelopathy in elderly people: a high incidence of conduction block at C3-4 or C4-5. *J Neurol Neurosurg Psychiatry* 1999; 66: 456-64.
- Tavy DL, Wagner GL, Keunen RW, Wattendorff AR, Hekster RE, Franssen H. Transcranial magnetic stimulation in patients with cervical spondylotic myelopathy: clinical and radiological correlations. *Muscle Nerve* 1994; 17: 235-41.
- Wilkinson M. The morbid anatomy of cervical spondylosis and myelopathy. *Brain* 1960; 83: 589-617.

Table 1. CMCT and SCEPs measurements (mean \pm SD (range))^a

shorter / longer CMCT (ms) (n = 24)

ADM 8.5 \pm 2.9 (3.6-16.5) / 11.5 \pm 3.3 (6.6-17.9)

AH 16.2 \pm 3.1 (10.6-22.0) / 18.4 \pm 3.3 (13.5-26.6)

SCEPs amplitude ratio of C6-7 to C2-3 (%) (n = 24)

25.7 \pm 21.0 (0-87.8)

SCEPs latency at C6-7 (ms) (n = 22)

4.3 \pm 0.4 (3.4-4.9)

^a CMCT, central motor conduction time; SCEPs, spinal cord evoked potentials; ADM, abductor digiti minimi; AH, abductor hallucis. Values from the two patients that failed to exhibit D-waves at the C6-7 intervertebral level were not included in the SCEPs latency data.

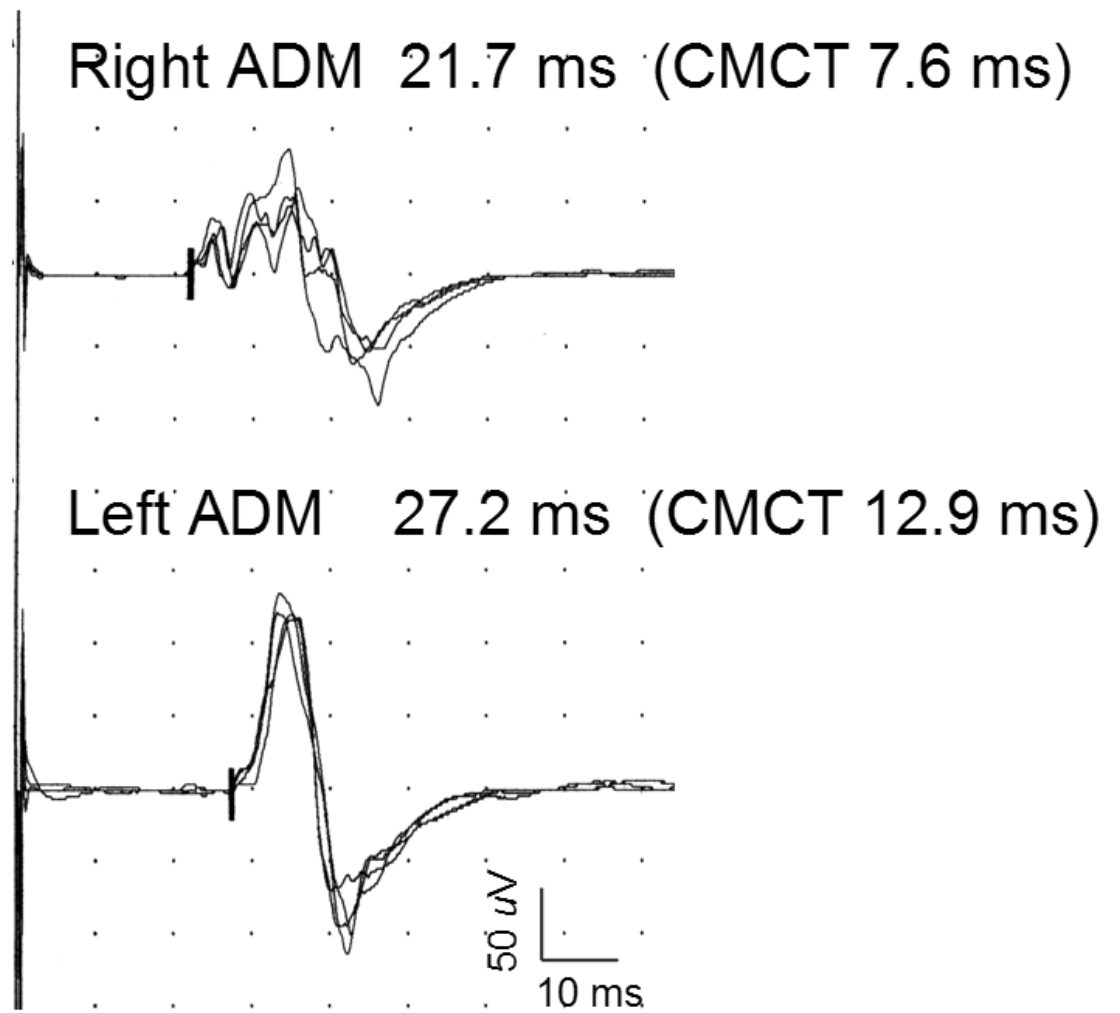


Fig.1-a

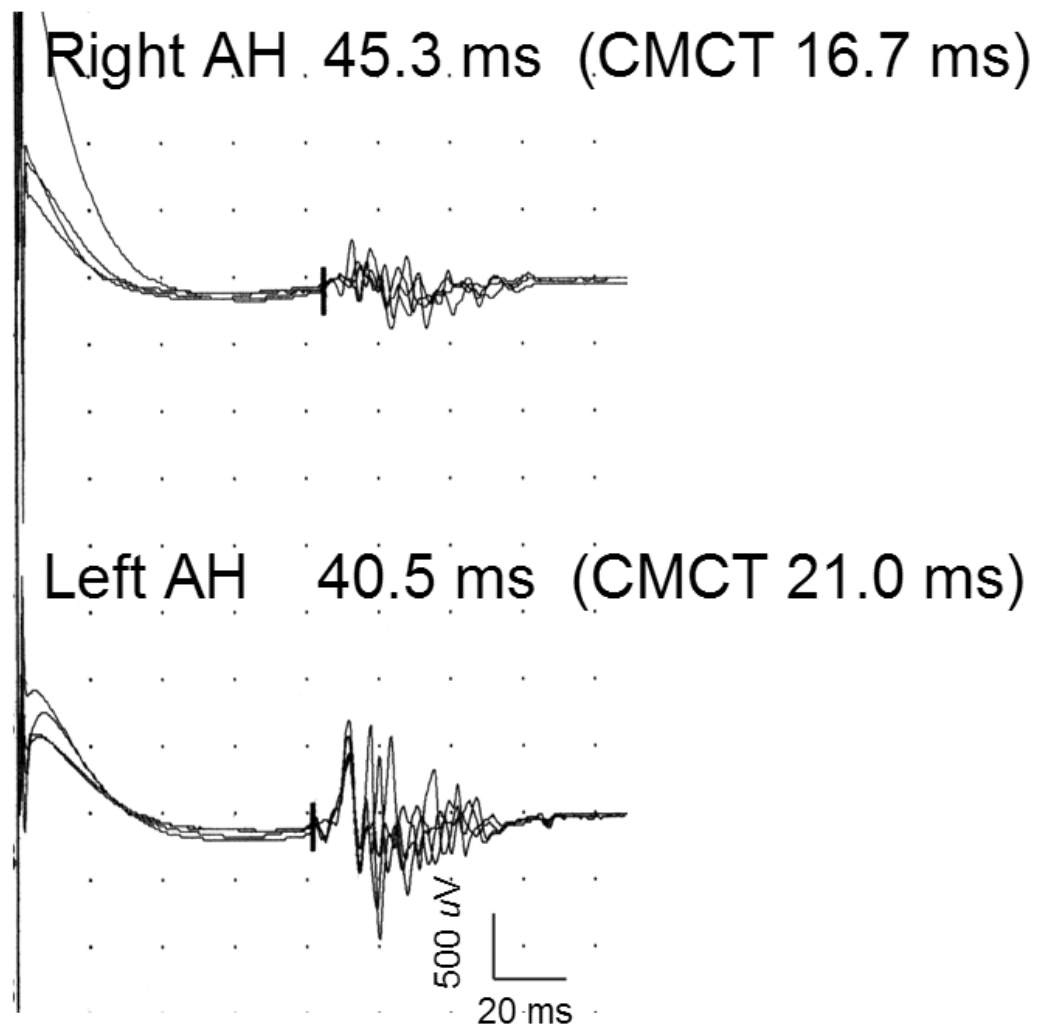


Fig.1-b

Stimulation

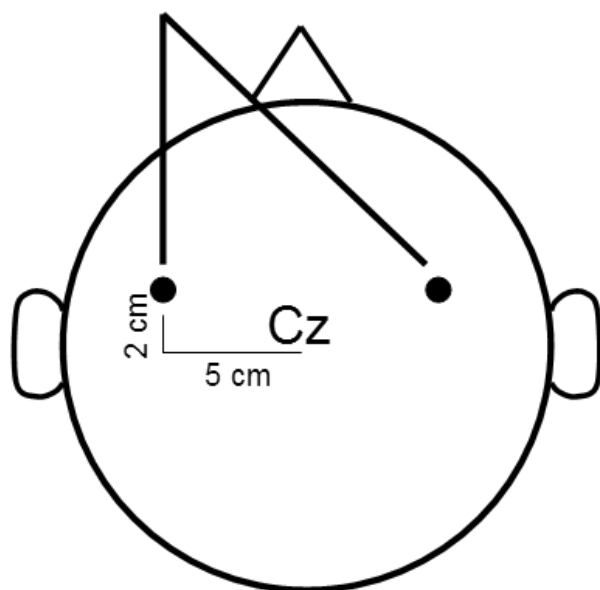


Fig.1-c

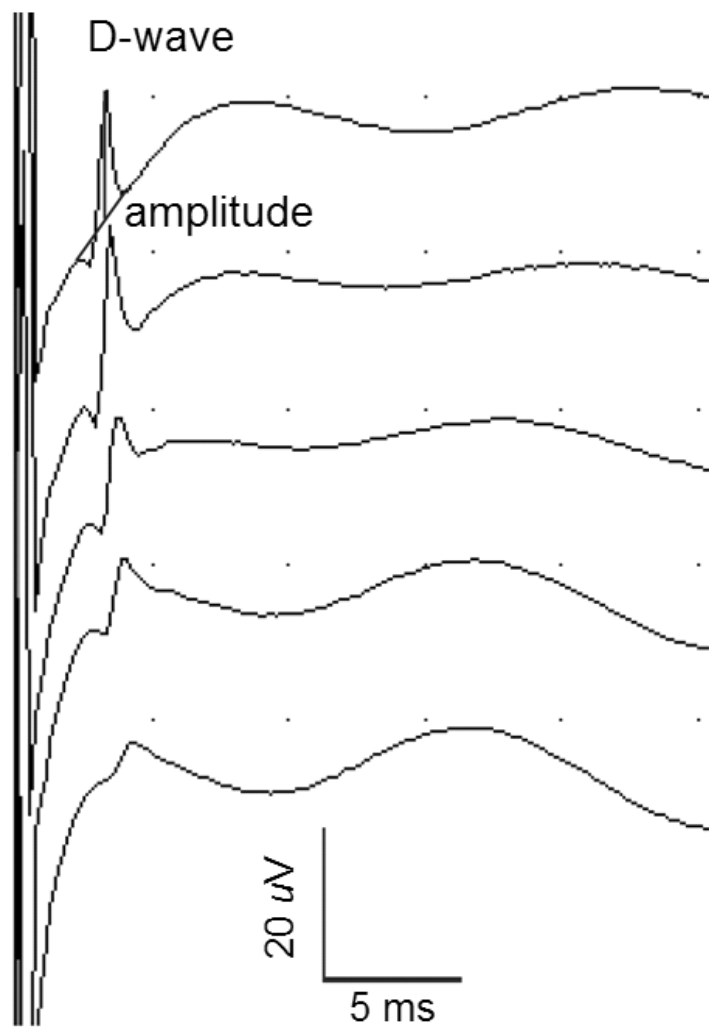


Fig.1-d

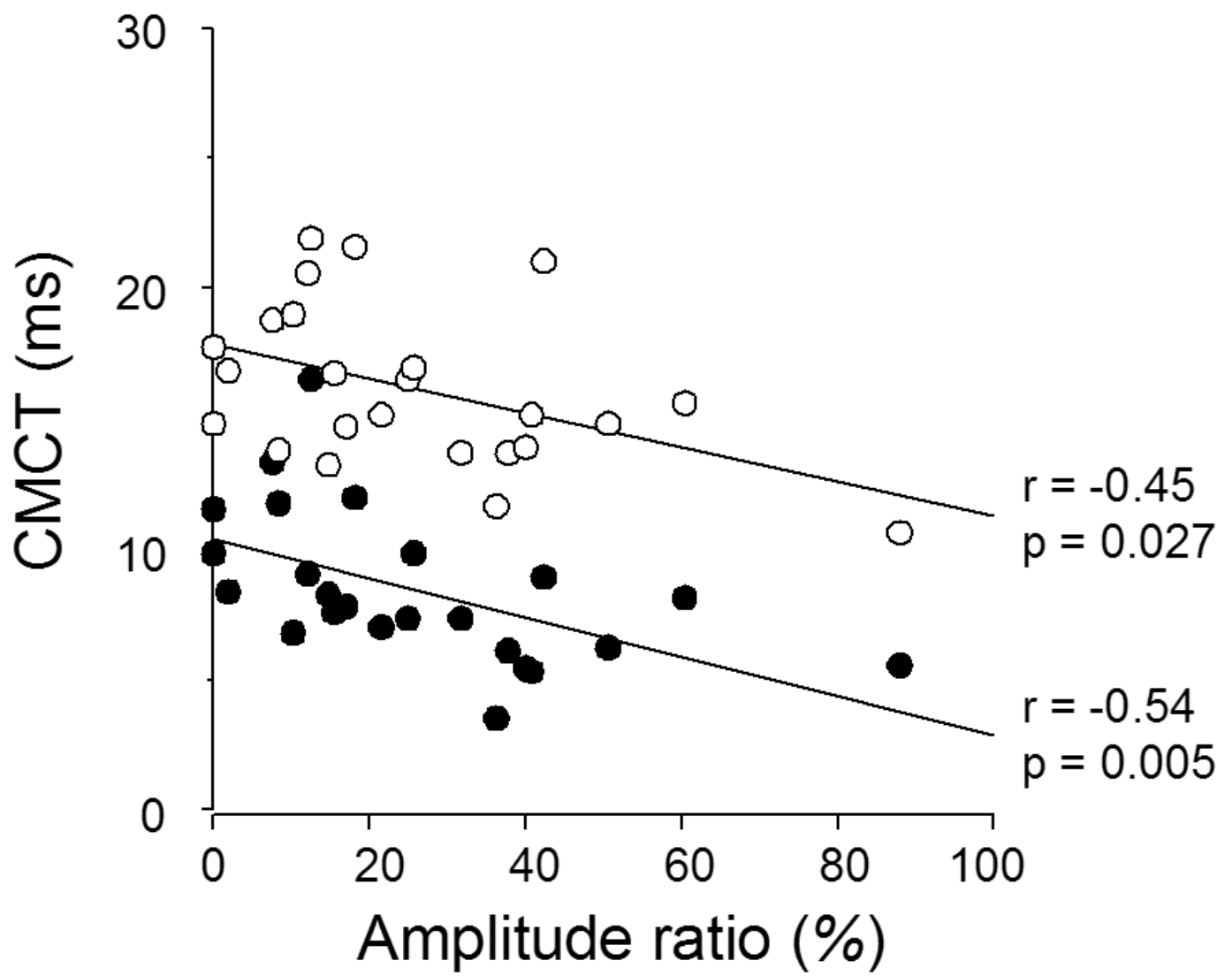


Fig.2-a

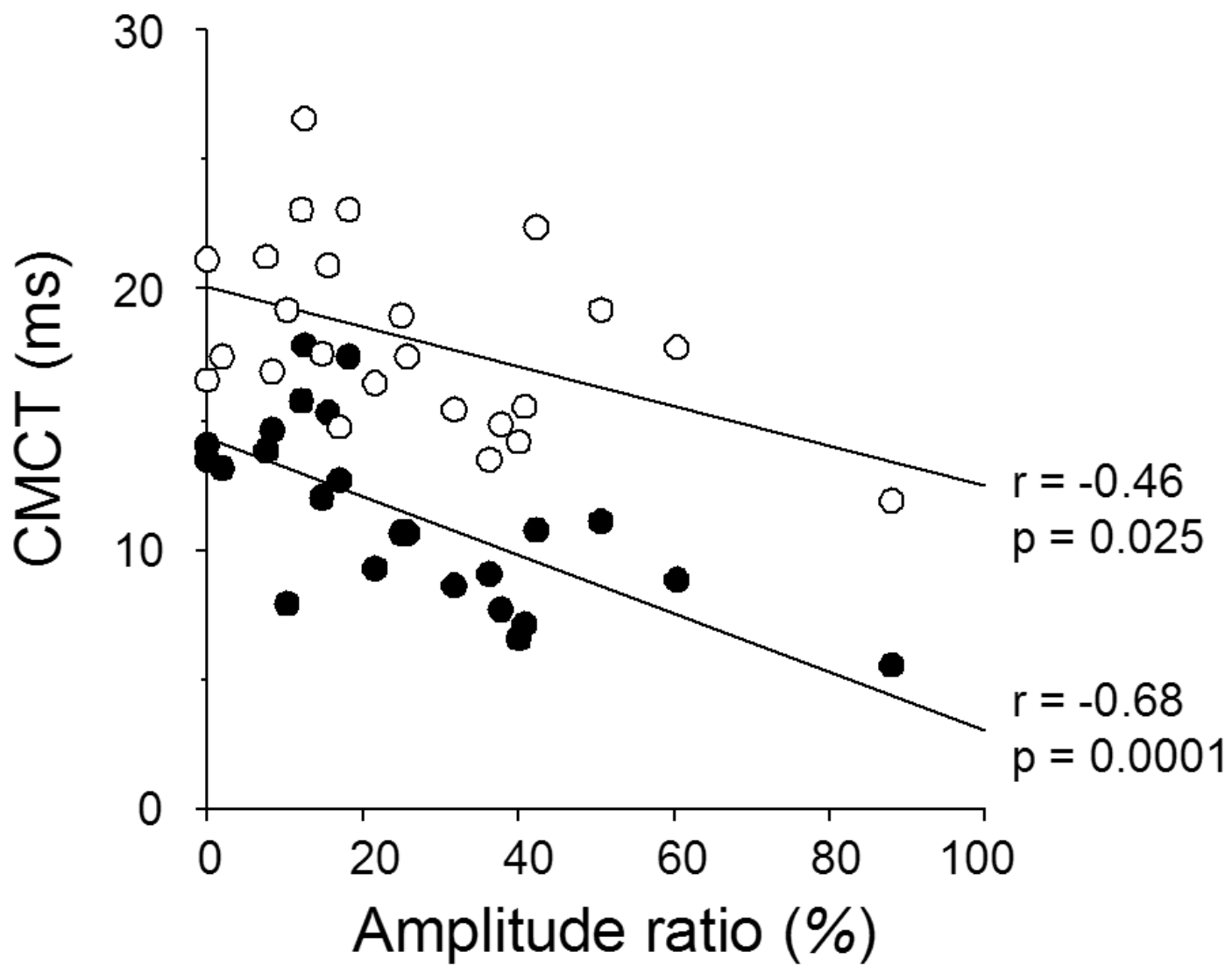


Fig.2-b

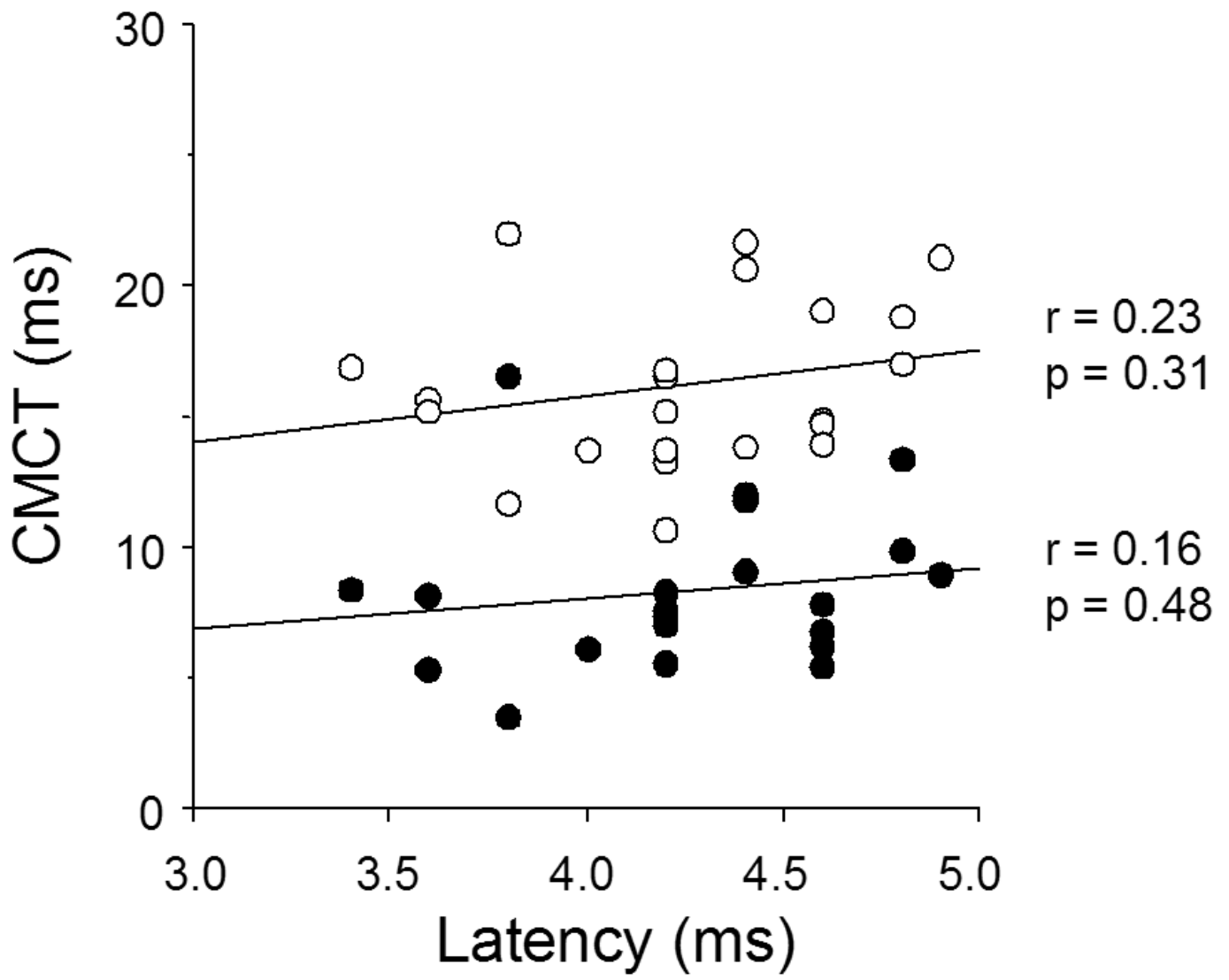


Fig.2-c

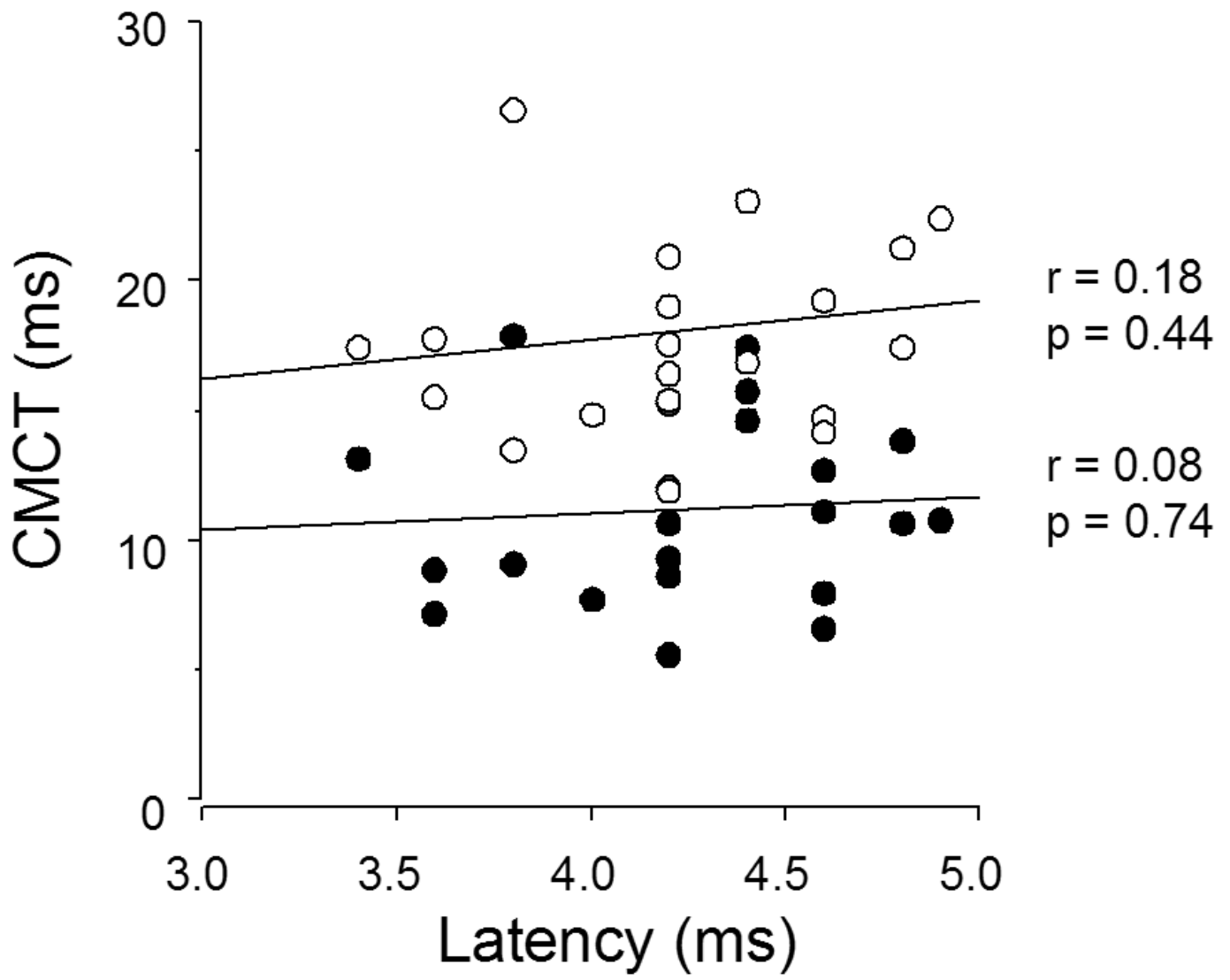


Fig.2-d